Time-dependent properties of a simplified Fermi-Ulam accelerator model

Denis Gouvêa Ladeira* and Jafferson Kamphorst Leal da Silva†
Departamento de Física, ICEx Universidade Federal de Minas Gerais Caixa Postal 702, 30.123-970, Belo Horizonte/MG, Brazil
(Received 23 June 2005; published 2 February 2006)

The chaotic low-energy region of a simplified Fermi-Ulam accelerator model is investigated numerically to determine the average energy and number of collisions as functions of time. We find that these properties exhibit scaling when the oscillation amplitude of the moving wall is small. Following a transient regime, the average energy increases in time, reaches a maximum and then shows a surprising slow decay.

DOI: 10.1103/PhysRevE.73.026201 PACS number(s): 05.45.Pq

I. INTRODUCTION

The Fermi accelerator is a dynamical system originally proposed by Fermi [1] to describe cosmic ray acceleration. Since then, different versions of this problem were proposed and studied by several authors. One of them is the so called Fermi-Ulam model (FUM) [2,3] that consists of a bouncing ball confined between a fixed rigid wall and a periodically moving one, representing an external time-dependent forcing. Without the external forcing the system is integrable; the time-dependent perturbation causes it to be nonintegrable. Although integrable and ergodic dynamical systems are reasonably well understood, quantitative descriptions of nonintegrable systems are still lacking. In particular, we still lack a deep understanding of how time-dependent perturbations affect the dynamics of Hamiltonian systems. Thus it is of interest to study such perturbations in simple systems.

The FUM may be described in terms of a two-dimensional measure-preserving map. We review the principal characteristics of this representation briefly. Of note is a set of invariant spanning curves in the phase space for high energy [3,4] that prevents unlimited growth of the energy (i.e., there is no Fermi acceleration). A chaotic sea involving a set of KAM islands is observed in the low-energy regime. As noted, when the amplitude of the moving wall is zero the system is integrable. As soon as the amplitude is different from zero, an integrable-chaotic transition occurs with the appearance of a chaotic sea [5]. This transition implies that average quantities are described by scaling functions when the collision number is an independent variable [6]. Finally, chaotic regions limited by two invariant spanning curves are observed at intermediate energies.

A version of this problem in a gravitational field is the so-called bouncer [7], which exhibits Fermi acceleration under certain conditions. The difference between the two models, as regards Fermi acceleration, was explained by Lichtenberg *et al.* [8]. Hybrid versions [9] involving the Fermi model and the bouncer and the Fermi model with energy dissipation [10] have also been studied. The quantum versions of these models have also been investigated in the literature [11–13]. It is worth mentioning that these one-dimensional classical systems allow direct comparison of theoretical results with experimental ones [14,15] and that the formalism used in its characterization can immediately be extended to the billiard class of problems [16–19].

In this work, we are interested in the chaotic sea of the simplified FUM. We study the average energy and average number of collisions as functions of *time*, and show that they are described by scaling functions when the amplitude of oscillations is small. Moreover, the exponents characterizing the scaling are different from those obtained when the collision number is the independent variable [6]; we were not able to find a relation between the two sets of exponents. We also determine the temporal evolution of the average energy. After a transient, it increases in time, reaches a maximum and then decays slowly at long times. This slow decay is surprising for two reasons. (i) When we consider the collision number n as the independent variable the average energy reaches a constant value when n is large. (ii) The first investigations of the FUM centered on the question of unbounded growth of the energy (Fermi acceleration), showing that this is not possible; here we have, at least for the simplified FUM, a *decreasing* average energy.

This paper is organized as follows. In next section we define the simplified FUM and the quantities of interest. In Sec. III we present and discuss our results. Finally, a summary is provided in Sec. IV.

II. THE SIMPLIFIED FUM

The one-dimensional Fermi-Ulam accelerator model describes the motion of a classical particle bouncing between two parallel rigid walls, one of which is fixed at the origin ($x=0$), while the other moves periodically in time. The position of the moving wall is given by $x_W(t'')=x_0+\varepsilon' \cos(wt''+\phi_0)$, where x_0 is the equilibrium position, ε' is the amplitude of oscillation, t'' is time, and w is frequency. After scale changes in time ($t'=t''w$) and in length $X_w=x_w/x_0$, we can work with nondimensional variables. In particular, we have that $X_W(t)=1+\varepsilon \cos(t'+\phi_0)$. Now, the only parameter of the system is $\varepsilon=\varepsilon'/x_0$. Note that the particle moves freely between impacts. We will describe the system by a map $T(V_n,\phi_n)=(V_{n+1},\phi_{n+1})$ which gives the velocity of the particle and the phase of the moving wall immediately after the particle suffers a collision with it. We will use a simplification [20] in our description. We will suppose that the "mov-

*Electronic address: dgl@fisica.ufmg.br
†Electronic address: jaff@fisica.ufmg.br

ing wall" is fixed but that, when the particle suffers a collision with it, the particle exchanges momentum as if the wall were moving. This simplification allows us to speed up our numerical simulations substantially as compared with the full model. It is valid when the velocity of the particle is larger than the wall velocity. Moreover, the structure of the phase space is essentially the same as that of the original model [5], with the chaotic sea in low-energy region, KAM islands surrounded by an ergodic sea, the position of the first invariant spanning curve, and existence of others chaotic regions limited by spanning curves in sufficiently high velocities. Incorporating this simplification in the model, the map is written as [2]

$$T=\begin{cases} V_{n+1}=|V_n-2\varepsilon\sin(\phi_{n+1})|, \\ \phi_{n+1}=\phi_n+\dfrac{2}{V_n} \bmod 2\pi. \end{cases} \quad (1)$$

The term $2/V_n$ specifies the time interval between two successive collisions of the particle with the "moving wall," while $-2\varepsilon\sin(\phi_{n+1})$ gives the corresponding fraction of velocity gained or lost in the collision in terms of the normalized amplitude ε of oscillation. The modulus in the equation is introduced to prevent the particle leaving the region between the walls.

Let us define $V^2(t')$ and $N(t')$ as the square velocity and the number of collisions at time t'. We are interested in the temporal evolution of the dimensionless energy ($E=2$ energy$/mx_0^2w^2$) and number of collisions (N) averaged over M realizations, characterized by initial phase values of the moving wall ϕ_0, randomly chosen in an interval I. This interval and the initial velocity V_0 must belong to the chaotic sea. If V_0 is small enough we have that $I=[0,2\pi)$. Moreover, we consider that the particle starts its motion from the moving wall position with velocity V_0. Namely,

$$E(t,\varepsilon,V_0)=\frac{1}{M}\sum_{j=1}^{M}V_j^2(t), \quad (2)$$

$$N(t,\varepsilon,V_0)=\frac{1}{M}\sum_{j=1}^{M}N_j(t), \quad (3)$$

where j refers to a realization. Note that these orbits, generated from (V_0,ϕ_0), belong to the chaotic sea. We define variable t as $t=t'-T_1$, where $T_1=2/V_0$ is the time of the first collision of the particle with the moving wall. In this way, we have that the time t starts at the first collision instant.

We are also interested in another kind of average. We first consider, for example, the average of the square velocity over the orbit generated from one initial phase ϕ_0

$$\bar{V}^2(t')=\frac{1}{t'}\int_0^{t'}V^2(\tau)d\tau. \quad (4)$$

Since the velocity is constant between two successive collisions, the integral in above equation is not difficult to solve. Then we consider an ensemble of M different initial phases

$$\bar{E}(t,\varepsilon,V_0)=\frac{1}{M}\sum_{j=1}^{M}\bar{V}_j^2(t). \quad (5)$$

Note that we have again set $t=t'-2/V_0$.

III. RESULTS

Let us first discuss some aspects related to the numerical simulations. Although time t is a continuous variable, we evaluate the averages defined in Eqs. (2), (3), and (5) at discrete, logarithmic spaced, values of t: $t_1,t_2,\ldots,t_N$. Note also that the map, defined in Eq. (1), give us the velocity after each collision with the moving wall and that the absolute value of the particle velocity is constant between two collisions with the moving wall. Suppose that we want to determine the energy at time t_1. We know that the particle is at the moving wall position with initial energy V_1^2 at $t=0$ and that the second collision occurs at $t_c=2/V_1$. We must consider the following procedure. (1) If $t_1\leqslant t_c$, the energy of the particle at t_1 will be $E_1=V_1^2$. (2) Else if $t_1>t_c$, a collision occurs at time $t=t_c=2/V_1$ and the particle has its velocity changed to V_1. Now the next collision time is given by $t_c=2/V_1+2/V_2$.

If case 1 is true we have determined the energy. Otherwise (case 2), we update the velocity and the next collision time. If now $t_1\leqslant t_c$ (case 1) the energy at t_1 is given by $E_1=V_2^2$. However, if t_1 is still larger than t_c, we repeat case 2, updating the two variables V and t_c. In fact, we repeat the complete procedure until t_1 becames larger than t_c. Then we update the energy variable. In this way we determine $E_1(t_1)$. A similar procedure is repeated for $t_2,\ldots,t_N$ with *appropriate* time intervals. We have just evaluated the energy $E_1(t)$ at the values t_1, $t_2,\ldots,t_N$ of time, for the first sample of the ensemble (particle 1).

Following the same lines, we can determine the values of the energy $E_2(t_1)$, $E_2(t_2),\ldots,E_2(t_N)$ for the second sample (particle 2 with a random initial phase). In this example, the ensemble average of the energy defined in Eq. (2) with $M=2$, can be written as $E(t_1)=[E_1(t_1)+E_2(t_1)]/2,\ldots,E(t_N)=[E_1(t_N)+E_2(t_N)]/2$. Each one of the other quantities $[N(t,\epsilon,V_0)$ and $\bar{E}(t,\epsilon,V_0)]$ can be numerically evaluated by a similar reasoning.

Let us now discuss the results obtained by numerical simulations. Figure 1(a) shows the behavior of the average energy $E(t,\varepsilon,V_0)$, when V_0 is small ($V_0\ll\varepsilon$) for four different values of the parameter ε. We see that the average energy is constant up to a time t_1, grows up to time t_2 and then decays slowly for large time. For $t\gg t_2$ we expect that the average energy behaves as

$$E(t,\varepsilon,V_0)\approx g(\varepsilon)t^{-\alpha}, \quad (6)$$

$$g(\varepsilon)\approx\varepsilon^{\beta}. \quad (7)$$

To obtain α, we first perform a best fit in the long time regime for each value of ε. For seven values of ε, varying from 5×10^{-5} up to 5×10^{-3} we find the minimum and maximum values of α are 0.043 ± 0.001 and 0.061 ± 0.001, respectively. Then we evaluate the average exponent. In order to

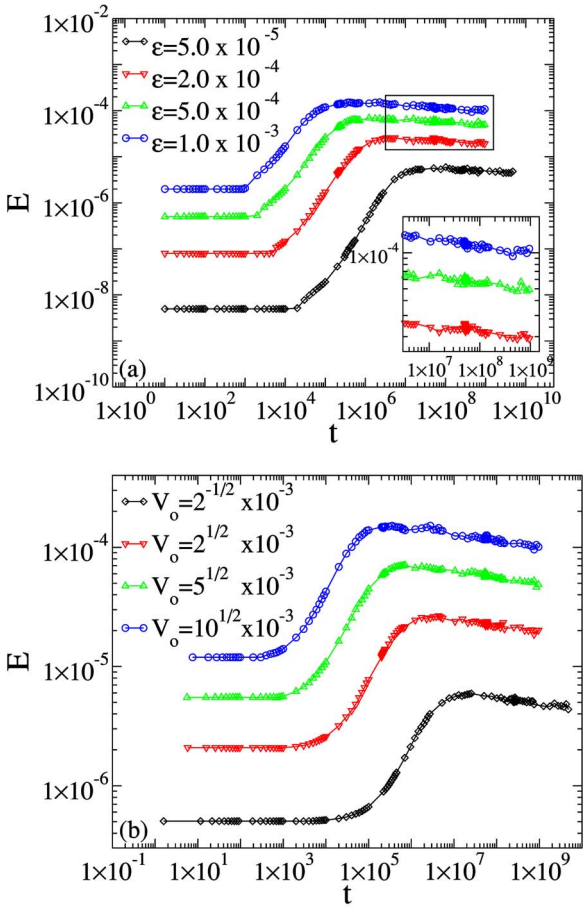

FIG. 1. (Color online) Log-log plots of the average energy $E(t)$ as a function of time t for (a) four values of the parameter ε and initial velocity $V_0=10^{-6}$ ($V_0 \ll \varepsilon$) and (b) four values of the parameter ε and four values of the initial velocity ($V_0 \gg \varepsilon$). We average over 2×10^4 realizations. The detail shows the slow decay of $E(t)$.

obtain β we consider plots of $E(t)t^{\alpha}$ vs t and determine the stationary value $g(\varepsilon)$ for different values of ε. A best fit of the plot $g(\varepsilon)$ vs ε furnishes the exponent β. An average over these seven values of ε yields $\alpha=0.055\pm0.005$ and $\beta=1.07\pm0.03$. We emphasize that the average energy decays in time. This happens because in each of the samples, the particle eventually has a very low velocity and remains for a long time $(2/V)$ with low energy. Therefore, at a time t, there are many realizations in which the particle has very low energy. These realizations are directly related to the time decay of the average energy. On the other hand, when we consider the number of collisions n as the independent variable [6], $E(n)$ approaches a constant value for large n. In the latter description, the time that the particle stays with a low velocity is not considered at all. High and low velocities play a similar role. We note also that t_2 varies with ε as

$$t_2 \approx \varepsilon^{-z}. \tag{8}$$

Therefore, performing a power law fit in the $t_2\times\varepsilon$ graph we obtain that $z=-1.49\pm0.02$.

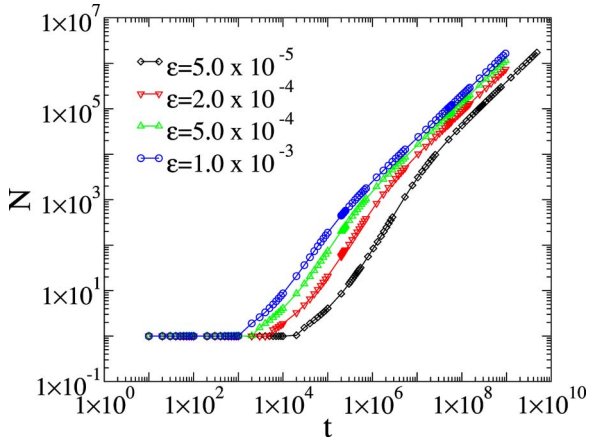

FIG. 2. (Color online) Log-log plot of the average number of collisions $N(t)$ vs t for four values of the parameter ε. The initial velocity is $V_0=10^{-6}$; average over 2×10^4 realizations.

A similar analysis can be done for the average number of collisions $N(t)$. From Fig. 2 we see that $N(t)$ grows in time. For $t \gg t_2$, its behavior can be described by

$$N(t,\varepsilon,V_0) \approx \varepsilon^{\delta} t^{\gamma}, \tag{9}$$

with $\gamma=0.943\pm0.001$ and $\delta=0.52\pm0.01$.

Before introducing a scaling description of the average energy, we must discuss the two characteristic times t_1 and t_2 evident in Fig. 1(a). In fact, t_1 is the time of the second collision, and is related to an initial transient. Therefore we have only one characteristic time t_2, separating two regimes. However, the power-law growth for $t \ll t_2$ is affected by the existence of t_1. Between t_1 and t_2 we have a crossover region, implying that it is almost impossible to determine the growth exponent. The behavior associated with t_1 can be estimated by a simple argument. After the first collision, which occurs at $t'=T_1=2/V_0$, we have that $V_1=-V_0+2\varepsilon\sin(T_1+\phi_0)$. Evaluating V_1^2 and taking the average in ϕ_0 we obtain $\langle V_1^2\rangle=2\varepsilon^2+V_0^2$. Making the approximation that $E \approx \langle V_1^2\rangle$, we obtain

$$E(t) \approx 2\varepsilon^2 + V_0^2. \tag{10}$$

Noting that $\langle V(t')\rangle$ can be very different from $\langle V_1\rangle=-V_0$ due collisions with the fixed wall, we approximate $\langle V(t')\rangle$ by $\sqrt{\langle V_1^2\rangle}$. Using $t_1=T_2-T_1=2/\langle V(t')\rangle$, we obtain

$$t_1 \approx \frac{2}{\sqrt{2\varepsilon^2 + V_0^2}}. \tag{11}$$

We can see in Fig. 1 that the energy curves do not change their values until the time of the second collision t_1, given by Eq. (11). After that new collisions occur and the energy curves have the initial growth. The above two equations can be used to determine the scaling exponents a_1, b_1, and c_1 defined by the scaling form of the average energy, namely,

$$E(t,\varepsilon,V_0) = lE(l^{a_1}t, l^{b_1}\varepsilon, l^{c_1}V_0). \tag{12}$$

Here l is the arbitrary scaling factor. When $V_0 \ll \varepsilon$, we obtain from Eqs. (10) and (11) that $E\sim\varepsilon^2$ and $t_1\sim\varepsilon^{-1}$. Choosing

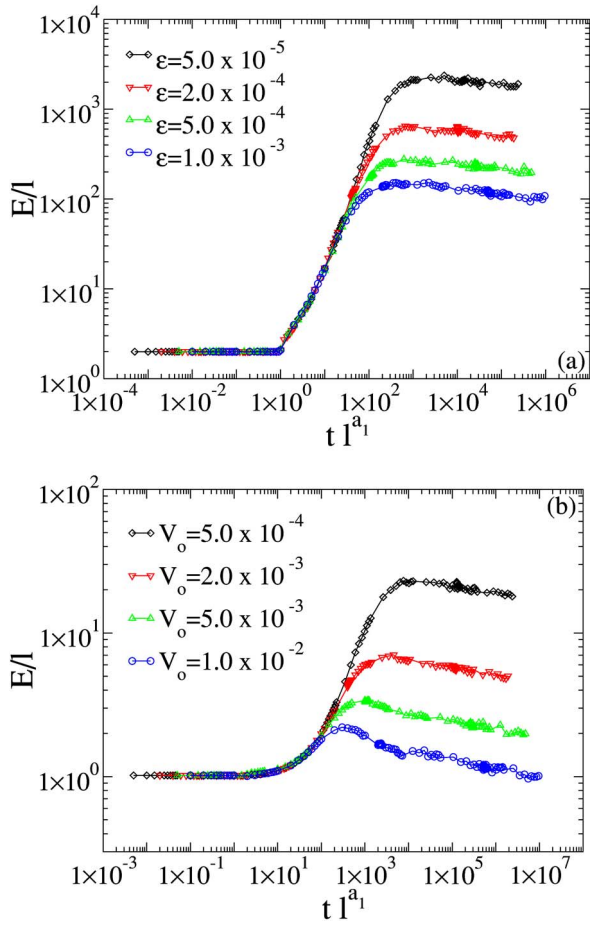

FIG. 3. (Color online) Log-log plot of the renormalized energy $E(t)/l$ as a function of renormalized time tl^{a_1} for four values of ε, when (a) the initial velocity is $V_0=10^{-6}\ll\varepsilon$ and (b) $V_0\gg\varepsilon$. We average over 2×10^4 realizations; $l=\varepsilon^{1/b_1}$, $a_1=1/2$, and $b_1=c_1=-1/2$.

$l=\varepsilon^{-1/b_1}$, Eq. (12) can be written as $E(t,\varepsilon,0)=\varepsilon^{-1/b_1}E(t/\varepsilon^{a_1/b_1},1,0)$. Therefore we have that $a_1/b_1=-1$ and $b_1=-1/2$. A similar analysis for $V_0\gg\varepsilon$ yields $c_1=-1/2$. In Fig. 1(a) we see the average energy for different ε when the initial velocity $V_0\approx0$. On the other hand, in Fig. 3(a) we see that these average energies collapse onto a universal curve with exponents defined above. The behavior of the average energy with ε for large velocities ($V_0\gg\varepsilon$), but still below the first spanning curve, is shown in Fig. 1(b). Using the same set of exponents we again obtain a collapse of the renormalized energies [see Fig. 3(b)]. Therefore the exponents $a_1=1/2$ and $b_1=c_1=-1/2$ described the scaling at short times.

In the limit $t\to\infty$ (or $t\gg t_2$), the energy obeys the scaling function given by Eq. (12) but with a different set of exponents, namely, a_2, b_2, and c_2. When $V_0\approx0$, we can choose $l=\varepsilon^{-1/b_2}$ to obtain $E(t,\varepsilon,0)=\varepsilon^{-1/b_2}f(\varepsilon^{-a_2/b_2}t)$. From Eq. (8) and the numerical results discussed just below that equation, we obtain $a_2/b_2=-1.49\pm0.02$. Since the energy decays slowly in the limit $t\gg t_2$ [see Eq. (6)], we may write $f(\varepsilon^{-a_2/b_2}t)\approx t^{-\alpha}\varepsilon^{-(a_2\alpha)/b_2}$. Therefore, we have that $\beta=-[(1/b_2)+(a_2/b_2)\alpha]$, $a_2=1.30\pm0.05$, and $b_2=-0.87\pm0.02$. In order to determine c_2 we use a result [5] connecting the simplified FUM to the standard model [2]. We transform the simplified map into a standard map by means of the coordinate change $I_n=2/V^*+2(V^*-V_n/V^{*2})$, where V^* is a typical mean velocity near to the lowest spanning curve, followed by a linearization around this value. We obtain the standard map equations $I_{n+1}=I_n-K_{\rm eff}\sin\phi_{n+1}$ and $\phi_{n+1}=\phi_n+I_n$, with an effective control parameter $K_{\rm eff}=4\varepsilon/V^{*2}$. The standard map has a transition from local to global chaos when $K=K_c\approx0.972$. It turns out that the maximum and minimum values of V^* in the lowest spanning curves furnish values of $K_{\rm eff}$ of the same order of magnitude of K_c, independent of ε. Thus $K_{\rm eff}$ can be written in terms of scaled variables $\varepsilon'=l^{b_2}\varepsilon$ and $V^{*\prime}=l^{c_2}V^*$. Assuming that $K_{\rm eff}$ is invariant [5] we obtain $b_2=2c_2$, which implies that the scaling exponent of the velocity is $c_2=-0.44\pm0.01$.

These exponents can also be determined via another procedure, in which we search for the best collapse of the average energy onto universal curves for long times. The cases $V_0\approx0$ and $V_0\neq0$ for the average energy as a function of ε are shown in Figs. 1(a) and 1(b), respectively. By renormalizing the variables we obtain a data collapse, as shown in Figs. 4(a) and 4(b), respectively.

It turns out that the exponents now are given by $a_2/b_2=-1.50\pm0.01$, $b_2=0.92\pm0.01$, and $c_2=0.46\pm0.01$. Note that the two sets of exponents have the same values to within uncertainty. We therefore take the average of the values obtained with the two different procedures to define our best estimates, namely, $a_2=1.35\pm0.05$, $b_2=-0.90\pm0.03$, and $c_2=-0.45\pm0.01$. These exponents describe the scaling in the long time regime.

The average number of collisions has a similar scaling form, namely, $N(t,\varepsilon,V_0)=lN(l^dt,l^e\varepsilon,l^fV_0)$. Choosing the scaling factor as $l=\varepsilon^{-1/e}$ and considering very low initial velocity, we have that $N\sim\varepsilon^{-1/e}f(t/\varepsilon^{d/e},1,0)$. Assuming that $f(t/\varepsilon^{d/e},1,0)\approx t^{\gamma}\varepsilon^{-(\gamma d)/e}$ when $t\gg t_2$ and that $d/e=a_2/b_2=-1.50\pm0.01$, we can compare this expression with Eq. (9) to obtain $e=2f=1.12\pm0.05$. The collapse of $N(t,\varepsilon,0)$ is shown in Fig. 5(a).

Finally let us discuss the decay for the energy, first averaged over the the orbit, and then averaged over the initial conditions as defined in Eq. (5). In Fig. 4(b) we show the slow decay of $\bar{E}$ for long times when $V_0\to0$ and $\varepsilon=5\times10^{-4}$. A power low best fit furnishes $\alpha=0.051\pm0.001$ with good correlation. Since the exponent α is small we cannot entirely discard a logarithmic decay.

IV. SUMMARY

Summarizing, we study the simplified Fermi-Ulam model when the time t is employed as the dynamical variable, instead of the variable n. As shown, this model presents two crossover times t_1 and t_2. By virtue of this property we have scaling laws with distinct sets of exponents. For the first crossover time, which governs the dynamical aspects of the average energy for small t values, we analytically established the exponent values $a_1=0.5$ and $b_1=c_1=-1/2$. For the second crossover time, which determines the behavior of the energy for large t, we established that $a_2=1.35\pm0.05$, $b_2=-0.90\pm0.03$, and $c_2=-0.45\pm0.01$. Using a_2, b_2, and c_2 we

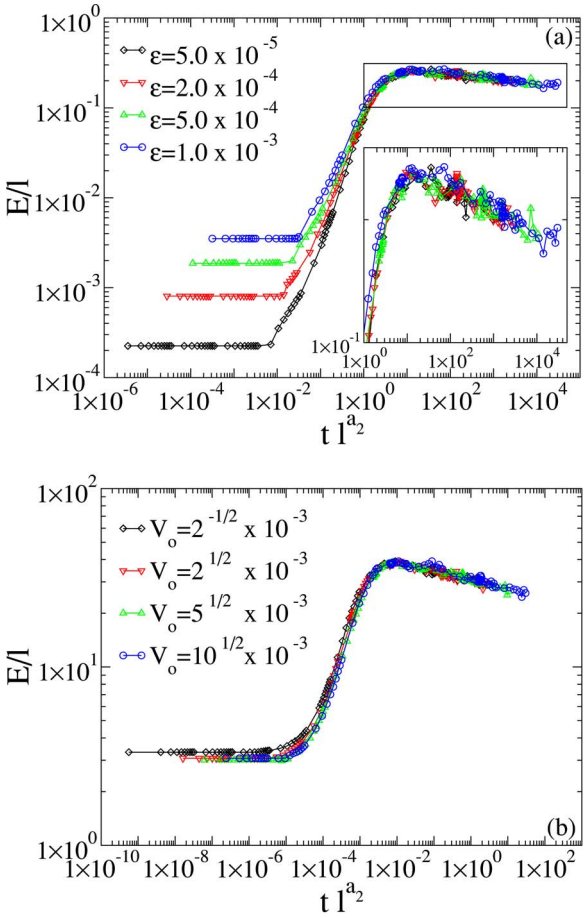

FIG. 4. (Color online) Log-log plot of the renormalized energy $E(t)/l$ as a function of renormalized time tl^{a_2} for four values of ε, when (a) the initial velocity is $V_0=10^{-6}\ll\varepsilon$ and (b) $V_0\gg\varepsilon$. $l=\varepsilon^{1/b_2}$, $a_2/b_2=-1.50\pm0.01$, $b_2=-0.92\pm0.01$, and $c_2=-0.46\pm0.01$; average over 2×10^4 realizations. Detail: Neighborhood of the maximum value of the renormalized energy.

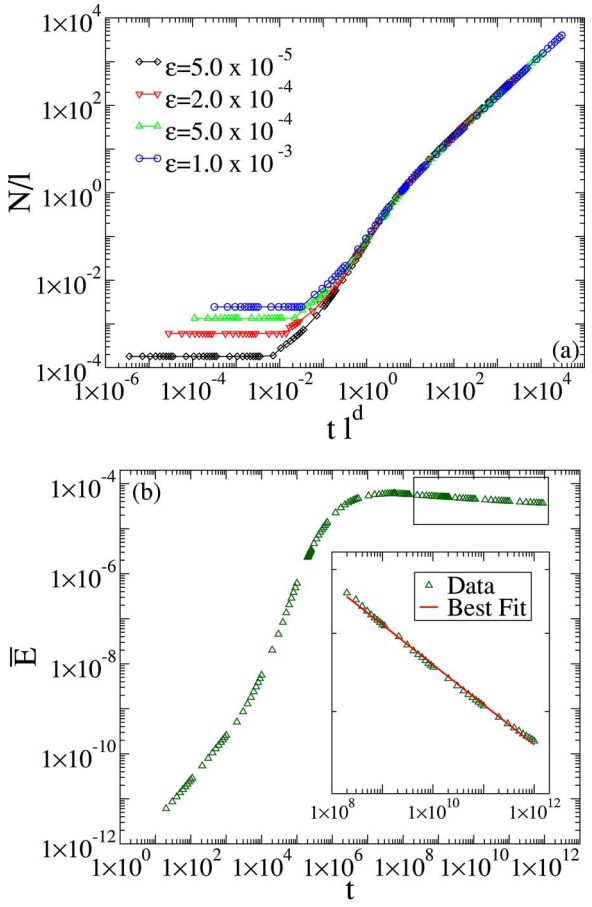

FIG. 5. (Color online) (a) Log-log plots of the renormalized number of collisions $N(t)/l$ as a function of renormalized time tl^d for four values of ε when the initial velocity is $V_0=10^{-6}\ll\varepsilon$. (b) Log-log plot of the energy first averaged over the orbit $\bar{E}(t,\varepsilon,V_0)$ when $V_0\to0$ and $\varepsilon=5\times10^{-4}$. Detail: Best power-law fit for the time decay, with $\alpha=0.051\pm0.001$ with correlation coefficient $r=-0.9991$.

obtain the collapse of the energy data when t is large. We emphasize that the scaling behavior holds only for small values of the renormalized amplitude ε. Moreover, this system presents another feature which has a brief and not difficult explanation. Eventually, a particle may collide with the moving wall and lose almost all its energy. When this happens, a very long time passes until the next collision and, for this reason, when $t\gg t_2$ the average energy decays slowly, as a power law with a small average exponent $\alpha=0.055\pm0.005$. This is surprising, since the asymptotic value of the average energy is constant when we consider the collision number n as the independent variable. The difference between the two descriptions is that high and low velocities play a similar role in the latter description.

ACKNOWLEDGMENTS

We thank Ronald Dickman for a careful reading of the manuscript. D.G.L. and J.L.K.S. were partially supported by Conselho Nacional de Pesquisa (CNPq). J.K.L.S. also thanks to the Fundação de Amparo à Pesquisa do Estado de Minas Gerais (FAPEMIG).

[1] E. Fermi, Phys. Rev. **75**, 1169 (1949).
[2] A. J. Lichtenberg and M. A. Lieberman, *Regular and Chaotic Dynamics*, Vol. 38 of Applied Mathematical Science (Springer Verlag, New York, 1992).
[3] M. A. Lieberman and A. J. Lichtenberg, Phys. Rev. A **5**, 1852 (1971).
[4] R. Douady, Ph.D. thesis, University Paris VII, Paris, 1982.
[5] E. D. Leonel, J. K. L. da Silva, and S. O. Kamphorst, Physica A **331**, 435 (2004).
[6] E. D. Leonel, P. V. E. McClintock, and J. K. da Silva, Phys.

Rev. Lett. **93**, 014101 (2004).
[7] L. D. Pustil'nikov, Trudy Moskov. Mat. Obsc. **34**, 1 (1977); L. D. Pustil'nikov, Theor. Math. Phys. **57**, 1035 (1983); L. D. Pustil'nikov, Sov. Math. Dokl. **35**, 88 (1987); L. D. Pustil'nikov, Sb. Russ. Acad. Sci. **82**, 231 (1995).
[8] A. J. Lichtenberg, M. A. Lieberman, and R. H. Cohen, Physica D **1**, 291 (1980).
[9] E. D. Leonel and P. V. E. McClintock, J. Phys. A **38**, 823 (2005).
[10] E. D. Leonel and P. V. E. McClintock, J. Phys. A **38**, L425 (2005).
[11] G. Karner, J. Stat. Phys. **77**, 867 (1994).
[12] S. T. Dembinski, A. J. Makowski, and P. Peplowski, Phys. Rev. Lett. **70**, 1093 (1993).
[13] J. V. José and R. Cordery, Phys. Rev. Lett. **56**, 290 (1986).
[14] Z. J. Kowalik, M. Franaszek, and P. Pieranski, Phys. Rev. A **37**, 4016 (1988).
[15] S. Warr, W. Cooke, R. C. Ball, and J. M. Huntley, Physica A **231**, 551 (1996).
[16] N. Saitô, H. Hirooka, J. Ford, F. Vivaldi, and G. H. Walker, Physica D **5**, 273 (1982).
[17] E. Canale, R. Markarian, S. O. Kamphorst, and S. P. de Carvalho, Physica D **115**, 189 (1998).
[18] A. Loskutov, A. B. Ryabov, and L. G. Akinshin, J. Phys. A **33**, 7973 (2000).
[19] A. Loskutov and A. B. Ryabov, J. Stat. Phys. **108**, 995 (2002).
[20] The simplified FUM was introduced by Lichtenberg and Lieberman and can be found, e.g., in Ref. [2].